

## INFLUENCE OF BSF THICKNESS AND AL-GETTERING STEPS ON IQE AND CELL PARAMETERS IN MC SI SOLAR CELLS

G. Hahn, P. Geiger, G. Schubert

University of Konstanz, Department of Physics, PO Box X916, 78457 Konstanz, Germany  
Tel: +49-7531-88-3644, Fax: +49-7531-88-3895. Email: giso.hahn@uni-konstanz.de

**ABSTRACT:** Al-alloying is an important step during solar cell fabrication. It can overcompensate the backside emitter, getter metal impurities and form a back surface field to reduce back surface recombination velocity. In this study we test the influence of different Al-alloying schemes on solar cell performance. Focus is laid on Al-gettering effect in combination with back surface passivation. For Edge-defined Film-fed Growth and String Ribbon material a significant increase in cell efficiency could be obtained by using screen-printing of Al paste and firing in comparison to evaporated Al and alloying. For the first time stable efficiencies under illumination in the 17-18% range could be reached for these materials (4 cm<sup>2</sup> cells). A reduced Al-gettering effect using screen-printing and firing can be detected by mapped lifetime measurements especially in good quality areas. The back surface recombination velocity can be reduced to about 300-600 cm/s in good quality areas of 3 Ωcm material. This can be measured by fitting spectral response and reflectivity data in the long wavelength part of the spectrum and is in good agreement with values predicted from theory.

**Keywords:** Back-Surface-Field - 1, Gettering - 2, Ribbon Silicon - 3

### 1 INTRODUCTION

Cost-effective multicrystalline (mc) silicon wafers for photovoltaic application suffer from defects reducing lifetimes of minority charge carriers. One possibility to enhance lifetimes during cell processing apart from hydrogenation are gettering steps. In recent publications it could be shown that especially low-cost ribbon silicon materials can benefit from these processing steps [1-5]. Lifetimes of up to 300 μs could be detected, but material quality is inhomogeneous even after optimised gettering and hydrogenation steps. As material quality in mc silicon wafers gets better, recombination at the cell's back side becomes important. Therefore, efficiencies of these cells are limited by the back surface recombination in the good quality areas of the cell. This paper will address the effect of several types of back surface fields (BSFs) obtained after evaporation and alloying on the one hand and screen-printing followed by a firing step on the other. Additionally, the effect of Al-gettering on material quality has been investigated.

Cell parameters of the processed cells using different types of gettering schemes have been measured and a detailed characterisation including mapped IQE (internal quantum efficiency) and spectral response has been performed. Lifetime mappings of the minority charge carriers have been carried out after removal of the metallization, BSF, and emitter. In this way information about the back surface recombination velocity can be gained as this parameter determines the IQE in the long wavelength range for a given lifetime.

### 2 CELL PROCESSING

Two crystalline ribbon silicon materials have been used for cell processing. Edge-defined Film-fed Growth (EFG) from RWE Schott Solar and Evergreen's String Ribbon (SR) silicon are both mc materials fabricated in large-scale production for solar cell processing. For this study 5.5 cm<sup>2</sup> wafers from both materials have been processed into 2.2 cm<sup>2</sup> solar cells according to the cell processes shown in Fig. 1.

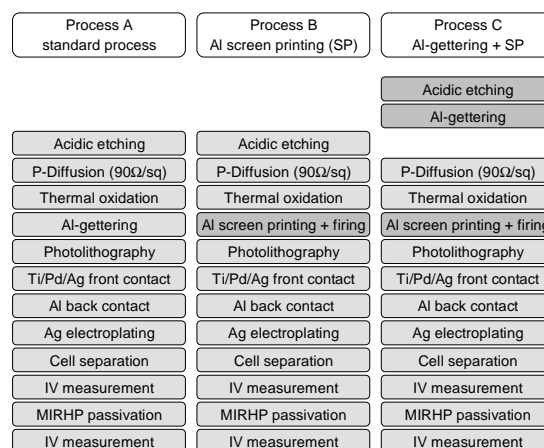


**Figure 1:** Solar cell processes used in this study.

Emitter formation is performed by POCl<sub>3</sub> diffusion in an open-tube furnace. Front surface passivation is applied by thermal oxidation of 15 nm of SiO<sub>2</sub>. Front contacts are formed by photolithography followed by electroplating to reduce series resistance. After cell separation by dicing cells can be characterised. Hydrogenation is carried out by microwave-induced remote hydrogen plasma (MIRHP) at 320 °C for 60 min.

In process A the BSF is formed by evaporation of 2 μm Al and alloying at 800 °C for 30 min. For process B Al paste is printed on the backside and a firing step in a belt furnace provides BSF formation. Firing is carried out using standard parameters as used for co-firing through SiN grown by plasma-enhanced chemical vapour deposition for industrial-type solar cells. As the short firing step (<60 s at temperatures above 600 °C) might result in less effective gettering, in process C we started cell processing by applying the same Al-gettering step as used in process A. The formed BSF was etched off prior to emitter diffusion and cells are afterwards processed according to process B. More details can be found in [5].

As EFG and SR material are of inhomogeneous as-grown quality but contain large grains in the direction of ribbon pulling, adjacent wafers in pulling direction reveal similar defect structures. To compare the impact of cell

processing, pairs of wafers adjacent in direction of pulling have been processed according to process A and B or B and C, respectively. Cell parameters for the best cells from each processing sequence and the effect of hydrogenation are described in detail in [5]. Cells from processes B and C show significantly higher values for short circuit current density  $J_{sc}$  and open circuit voltage  $V_{oc}$ . Evaporation of an additional ZnS/MgF<sub>2</sub> antireflection coating results in stable efficiencies for the best cells of 17.7% (SR) and 16.7% (EFG) [5].

### 3 MAPPED INTERNAL QUANTUM EFFICIENCY

Mapped internal quantum efficiencies (IQE) at 980 nm for two adjacent SR cells fabricated according to process A and B after hydrogenation can be seen in Fig. 2. Clearly visible are the similar grain structures. The BSF fabricated by screen-printing in process B leads to a higher IQE in good quality areas (compare regions 2 and 4), causing the higher  $J_{sc}$ .

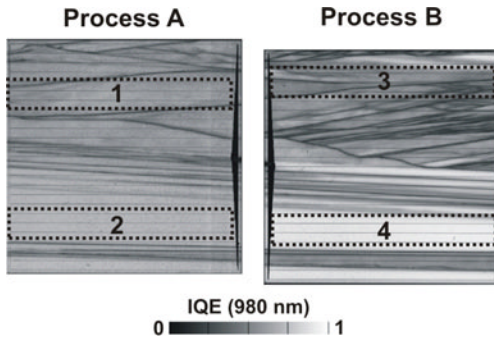


**Figure 2:** IQEs at 980 nm of two adjacent SR cells fabricated according to processes A and B.

The comparison between processes B and C is shown in Fig. 3, again for two adjacent SR cells. No significant difference can be seen, but there is a tendency towards a higher IQE in good quality areas for process C (more details in [5]).

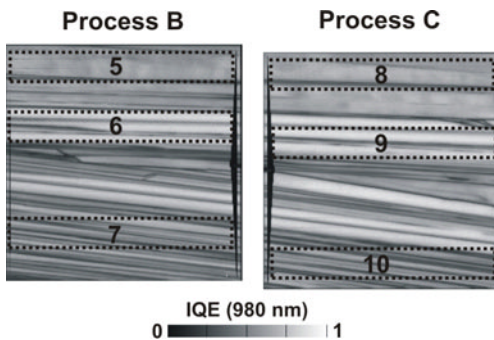


**Figure 3:** IQEs at 980 nm of two adjacent SR cells fabricated according to processes B and C.

Additionally, spectral response has been measured on the four cells shown in Fig. 2 and Fig. 3. During these measurements illumination area was either 2.2 cm<sup>2</sup> to measure the integral value for the whole cell, or 0.25-2 cm<sup>2</sup> by using a shadow mask to measure values integrated within the areas indicated in Fig. 2 und Fig. 3.

These measurements are used for fitting procedures presented in section 5.

### 4 MAPPED LIFETIMES

For considerations of the effective back surface recombination velocity  $S_{eff}$  the local minority charge carrier bulk lifetime  $\tau_b$  is an important parameter. As material quality is inhomogeneous even after cell processing, a mapped method has to be chosen. We used microwave-detected photoconductance decay ( $\mu$ PCD), with an illuminated spot size <1 mm for measurement in low injection conditions. After removing metal contacts and etching of emitter and BSF, samples were cleaned and immersed in iodine/ethanol solution to suppress surface recombination. As lifetimes cover a wide range in areas of different quality, special care has to be taken in order to obtain correct values in all regions. Therefore several measurements with different time ranges have to be carried out and combined [3]. In Fig. 4 the results of the obtained mappings are shown and can be compared directly with Fig. 2 and Fig. 3.

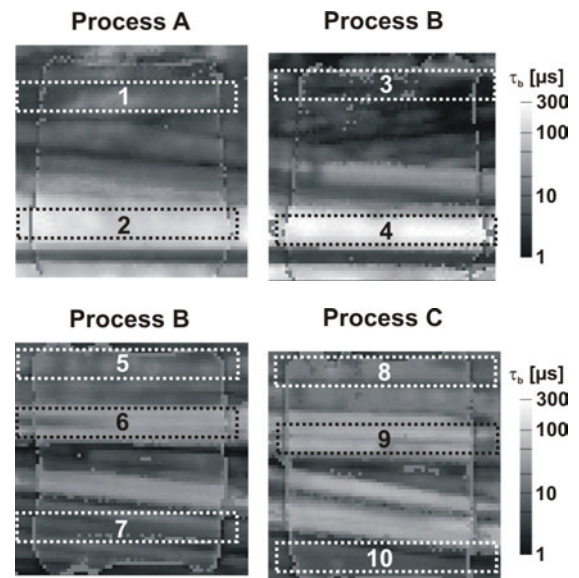


**Figure 4:** Lifetime mappings of the cells presented in Fig. 2 and Fig. 3 after removing metals contacts, BSF, and emitter.

Comparing  $\tau_b$  for process B and C (Fig. 4, bottom) no significant benefit from the additional Al-gettering step in process C can be detected, although  $\tau_b$  seems to be higher in good quality areas (Tab. 1). This tendency could be seen in most cells investigated within this study. If metals are present in low quality areas, then they might be in form of precipitates that can not be dissolved easily during the 800 °C 30 min gettering step of process A.

Comparing results of IQE and  $\tau_b$  for process A and B it is obvious that high lifetimes well above 100  $\mu$ s in area 2 as detected after etching did not result in a high IQE on cell level due to the high  $S_{eff}$ . But high lifetimes do result in high IQEs for process B because of the lower  $S_{eff}$  (region 4). Similar results have been obtained for EFG [5].

## 5 BACK SURFACE RECOMBINATION VELOCITY

### 5.1 BSF thickness

The effectiveness of the Al BSF is dependent on its thickness and doping concentration [6]. BSF thickness is mainly influenced by the thickness of the Al layer present prior to alloying and the peak temperature during alloying/firing. The resulting thickness and concentration can in principle be calculated according to the Al/Si phase diagram. Al-BSF thicknesses for the cells presented in Fig. 2 and Fig. 3 have been measured after etching in HF:HNO<sub>3</sub>:CH<sub>2</sub>COOH (1:3:6) for 15 s using optical microscopy and scanning electron microscopy (SEM). Measured BSF thickness for process A is below 1 μm whereas measured thickness for processes B and C is between 8-10 μm (Fig. 5). Electrochemical capacitance voltage (ECV) measurement on a SR sample revealed peak concentrations around 6-7·10<sup>18</sup> cm<sup>-3</sup> in the BSF (Fig. 6).

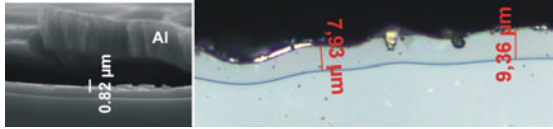


**Figure 5:** BSF thickness of cells shown in Fig. 2. Left: process A (SEM), right: process B (optical microscope).

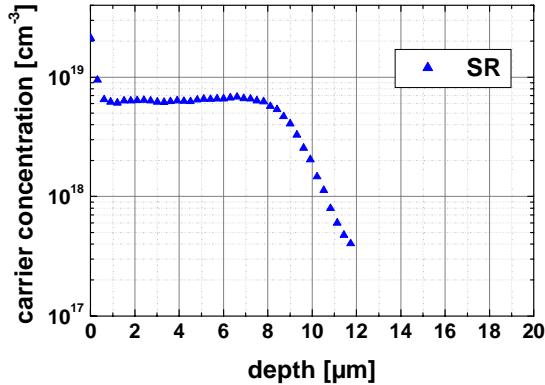


**Figure 6:** ECV measurement of the BSF region for a SR sample.

### 5.2 Determination of $S_{eff}$

The effect of the BSF is often modelled through the use of an effective back surface recombination velocity  $S_{eff}$ , which is defined at the edge of the quasi-neutral region of the base. In this approach the highly doped BSF is substituted by a quasi-surface with a surface recombination velocity  $S_{eff}$ . In principle, for a homogenous doped BSF  $S_{eff}$  can be calculated using equation (1) [7]

$$S_{eff} = \frac{N^+ D^+ \frac{S_b L^+}{D^+} + \tanh\left(\frac{W_{BSF}}{L^+}\right)}{1 + \frac{S_b L^+}{D^+} \tanh\left(\frac{W_{BSF}}{L^+}\right)} \quad (1)$$

with doping concentration  $N^+$ , diffusion constant of minority carriers  $D^+$  and minority carrier diffusion length  $L^+$  in the BSF region, a surface recombination velocity at the physical back surface  $S_b$ , a thickness of the BSF  $W_{BSF}$

and a doping concentration in the base  $N$ . The BSF parameters are, however, very difficult to determine and vary for different BSF types. Therefore other methods based e.g. on lifetime measurements have been applied to test structures [6,8,9]. In this study we determined  $S_{eff}$  experimentally by a method proposed and introduced by Fischer [8]. The measured IQE was fitted in the medium to long wavelength range to obtain the relevant parameters to calculate  $S_{eff}$  using the following equation

$$S_{eff} = \frac{D L - L_{eff} \tanh(W/L)}{L L_{eff} - L \tanh(W/L)} \quad (2)$$

where  $D$  is the diffusion constant of minority carriers,  $L$  the minority carrier diffusion length,  $L_{eff}$  the effective diffusion in the bulk and  $W$  the cell thickness. This method circumvents the characterization of internal BSF parameters and allows characterization of areas varying in quality in mc Si. Moreover, the method can be applied to processed cell structures. As in the relevant wavelength range back side reflection and absorption play a significant role, the measured reflectivity was, in a first step, fitted to obtain the back side reflection  $R_b$  and the fraction of diffuse rear surface reflection (Lambertian factor) following the approach of Brendel [10]. In a next step  $L_{eff}$  was obtained by a fit according to the method proposed by Basore [11] in the medium wavelength range (760-920 nm). The IQE of the long wavelength range was used to determine  $L$ . As stated above, the IQE in this wavelength range is dominated by rear side properties, thus  $L$  determination is very critical. In Fig. 7 and 8 the measured IQEs and reflectivities of process A and B cells

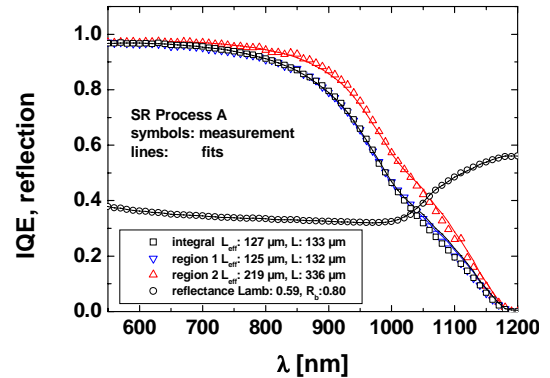


**Figure 7:** IQE data of the cell shown in Fig. 2, left (process A). Rear side recombination dominates the IQE in the medium to long wavelength range.

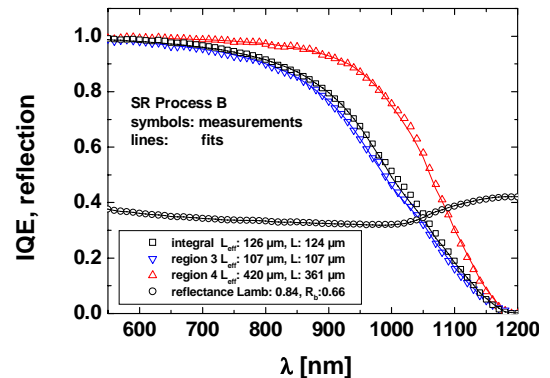


**Figure 8:** IQE data of the cell shown in Fig. 2, right (process B). Rear side recombination is reduced.

as well as the corresponding fitting curves are presented. Fitted  $L_{eff}$ ,  $L$  and  $S_{eff}$  values of all cells for the integral cell as well as for specified regions (Fig. 2 and Fig. 3) are given in Table 1.

The procedure to obtain  $S_{eff}$  used in this work has to be discussed carefully.  $L$  determination is difficult as explained above. Moreover, the error in  $S_{eff}$  increases dramatically in regions where  $L < W$ , because here  $S_{eff}$  is very sensitive to changes in  $L$  (see equation (2)). Another critical parameter is the bulk diffusion constant  $D$ , which is unknown for different grains of a mc-silicon substrate. It is reasonable to choose an upper bound of  $D_{up}=30 \text{ cm}^2/\text{s}$  being the simulated value for a monocrystalline 3  $\Omega\text{cm}$  Si substrate. As a lower bound for defect-rich mc Si  $D_{low}=20 \text{ cm}^2/\text{s}$  was chosen. To show the limitations of this method in Table I a lower bound for  $L$  ( $L_{min}$ , no recombination at the rear side) and the best fit  $L$  ( $L_{best \text{ fit}}$ ) together with the corresponding  $S_{eff}$  calculated using  $D_{up}$  and  $D_{low}$  is shown. In regions with a high lifetime  $D=30 \text{ cm}^2/\text{s}$  should be more accurate.

Nevertheless this method proved to be useful for regions with  $L \geq W$  to get an estimation for the quality of the BSF. The rear side passivation of process A is less effective as compared to process B.  $S_{eff}$  in good regions is significantly higher than the effective rear side recombination obtained with process B. With this method  $S_{eff}$  values of 300-600 cm/s were determined for a screen-printed Al-BSF in good quality areas. These are somewhat higher values than those published by Fischer [8] and Lölgen [6], but both applied an additional HF cleaning step before Al printing.

A similar process sequence with the same back side formation led to record high efficiencies in the 18-19% range for tri-crystalline silicon (TriSi) [12]. This indicates the possible potential for BSF formation using Al-paste in combination with standard co-firing conditions.

**Table I:** Summary of obtained data for areas indicated in Fig. 2, Fig. 3, Fig. 4, and for the whole cell (area: int)

area	$L_{eff}$ [ $\mu\text{m}$ ]	$L_{min} / L_{best \text{ fit}}$ [ $\mu\text{m}$ ]	$S_{eff, \text{ bestfit}}$ [cm/s] $D=20 / D=30$
1	125	120 / 132	$2.56 \cdot 10^4 / 3.85 \cdot 10^4$
2	219	185 / 336	6360 / 9540
int	127	121 / 133	$1.07 \cdot 10^4 / 1.6 \cdot 10^4$
3	107	104 / 107	1870 / 2800
4	420	282 / 361	318 / 478
int	126	121 / 124	757 / 1140
5	123	118 / 123	1630 / 2440
6	151	140 / 144	370 / 556
7	80	79.5 / 79.8	1080 / 1620
int	100	98 / 100	2000 / 3000
8	152	141 / 148	730 / 1100
9	196	120 / 177	211 / 317
10	75	74.7 / 75	2670 / 4000
int	126	121 / 123.5	669 / 1000

## 6 SUMMARY

The influence of BSF formation on cell parameters has been tested on solar cells made from EFG and SR silicon. 2.2  $\text{cm}^2$  cells have been processed using adjacent wafers according to 3 processes. Process A based on evaporation of 2  $\mu\text{m}$  Al and alloying results in BSF thickness  $< 1 \mu\text{m}$  and  $S_{eff}$  limits IQE in good quality areas.

Processes B and C with BSFs formed via deposition of Al paste followed by firing revealed higher IQEs in good quality areas due to lower  $S_{eff}$ . The additional Al-pregettering step in process C results in a tendency towards higher lifetimes in good quality areas only. Efficiencies in the 17-18% range could be obtained as described in detail elsewhere [5].

A method was presented to obtain values for  $S_{eff}$  in areas of different material quality of the processed solar cells.  $S_{eff}$  of around 300 cm/s could be reached on 3  $\Omega\text{cm}$  SR material in good quality regions using processes B and C based on screen-printing. There is a tendency towards higher values for lower quality areas, but the method used for fitting is highly sensitive to the diffusion length. Lower diffusion lengths lead to a high inaccuracy in the determination of  $S_{eff}$ . The same sequence for BSF formation using Al screen-printing for back side metallization led to efficiencies in the 18-19% range for 5  $\Omega\text{cm}$  TriSi material [12].

## 7 ACKNOWLEDGEMENTS

We like to thank M. Keil for assistance during cell processing and A. Metz from RWE Schott Solar as well as A.M. Gabor from Evergreen Solar for material supply. Part of this work was supported within the ASIS program by the German BMU under contract number 0329846J.

## 8 REFERENCES

- [1] J-W. Jeong, A. Rohatgi, M.D. Rosenblum, J.P. Kalejs, Proc. 28<sup>th</sup> IEEE PVSC, Anchorage 2001, 83
- [2] V. Yelundur, A. Rohatgi, J.-W. Jeong, A.M. Gabor, J.I. Hanoka, R.L. Wallace, Proc. 28<sup>th</sup> IEEE PVSC, Anchorage 2001, 91
- [3] P. Geiger, G. Kragler, G. Hahn, P. Fath, E. Bucher, Proc. 29<sup>th</sup> IEEE PVSC, New Orleans 2002, 186
- [4] G. Hahn, A. M. Gabor, Proc. 3<sup>rd</sup> WC PVSEC, Osaka 2003, 1289
- [5] G. Hahn, P. Geiger, Progr. Photovolt. Res. Appl. 11 (2003) 341
- [6] P. Lölgen, Surface and volume recombination in silicon solar cells, PhD thesis, University of Utrecht (1995)
- [7] M.P. Godlewski, C.R. Baraona, H.W. Brandhorst, Proc. 10<sup>th</sup> IEEE PVSC, Palo Alto 1973, 40
- [8] B. Fischer, Loss analysis of crystalline silicon solar cells using photoconductance and quantum efficiency measurements, PhD thesis, University of Konstanz (2003)
- [9] A. Metz, S. Dauwe, L. Mittelstädt, S. Steckemetz, R. Hezel, Proc. 17<sup>th</sup> EC PVSEC, Munich 2001, 1913
- [10] R. Brendel, Thin-Film Crystalline Silicon Solar Cells (Wiley-VCH, Weinheim, 2003)
- [11] P.A. Basore, IEEE Trans. Electron Devices ED-37 (1990) 337
- [12] D. Sontag, G. Hahn, I. Melnyk, A. Hauser, P. Fath, E. Bucher, W. Krühler, Proc. 3<sup>rd</sup> WC PEC, Osaka 2003, 1304